

Accepted Manuscript

Discussion on Graphical Methods to Identify Point Sources from wind and Particulate Matter-Bound Metal Data

Sara Ruiz Andrés, Ignacio Fernández-Olmo, Ángel Irabien Gullias

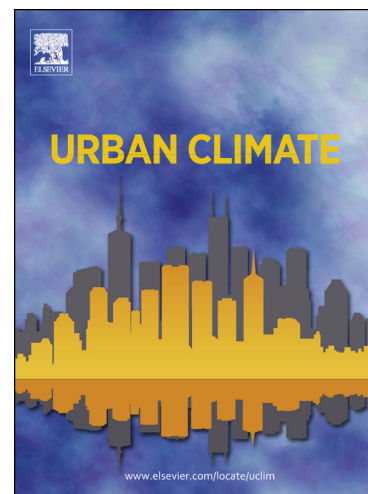
PII: S2212-0955(13)00057-6
DOI: <http://dx.doi.org/10.1016/j.uclim.2013.11.001>
Reference: UCLIM 53

To appear in:

Received Date: 30 April 2013
Revised Date: 10 October 2013
Accepted Date: 8 November 2013

Please cite this article as: S.R. Andrés, I. Fernández-Olmo, Á.I. Gullias, Discussion on Graphical Methods to Identify Point Sources from wind and Particulate Matter-Bound Metal Data, (2013), doi: <http://dx.doi.org/10.1016/j.uclim.2013.11.001>

This is a PDF file of an unedited manuscript that has been accepted for publication. As a service to our customers we are providing this early version of the manuscript. The manuscript will undergo copyediting, typesetting, and review of the resulting proof before it is published in its final form. Please note that during the production process errors may be discovered which could affect the content, and all legal disclaimers that apply to the journal pertain.



**DISCUSSION ON GRAPHICAL METHODS TO IDENTIFY POINT SOURCES
FROM WIND AND PARTICULATE MATTER-BOUND METAL DATA**

by

Sara Ruiz Andrés

Department of Chemical Engineering and Inorganic Chemistry
Cantabria University, Santander, Spain.
ruizas@unican.es, +34 942201579

Ignacio Fernández-Olmo*

Department of Chemical Engineering and Inorganic Chemistry
Cantabria University, Santander, Spain.
fernandi@unican.es, +34 942206745

and

Ángel Irabien Gullias

Department of Chemical Engineering and Inorganic Chemistry
Cantabria University, Santander, Spain.
irabienj@unican.es, +34 942201597

*corresponding author

DISCUSSION ON GRAPHICAL METHODS TO IDENTIFY POINT SOURCES FROM WIND AND PARTICULATE MATTER-BOUND METAL DATA

Abstract

The aim of the present work is to use graphical methods based on the evaluation of selected trace metals (Mn, Cu, Cr, V and Ni) and wind direction monitoring data to identify sources of trace metal in the main urban areas of the Cantabria Region (Northern Spain). These graphical methods take into account the frequency of wind in each sector and the measured concentration of trace elements in PM₁₀. The comparison between the contribution of wind and selected trace metals to each sector is presented in polar diagrams. The main conclusions derived from these diagrams are compared to those obtained from radial diagrams based on pollutant concentration roses computed from daily metal levels and hourly wind direction data. The procedure, based on plotting the ratio between the contribution of trace metals and wind data to each sector on polar diagrams, may result in an easier interpretation. Finally, both procedures are applied to data from three sampling sites located in Santander Bay, to study the influence of point sources on the levels of Mn. The analysis of the results shows that similar conclusions were obtained from both methods. These methods are primarily recommended when large emissions are produced by local point sources.

Keywords: trace metal, pollutant concentration rose, wind direction, graphical method

1. Introduction

The levels and composition of particulate matter (PM) are directly linked to the proven adverse effects on human health [1]. The levels of suspended particulate matter with an aerodynamic diameter less than 10 μm (PM₁₀) in some European areas usually exceed the yearly and daily limit values of 40 and 50 $\mu\text{g}/\text{m}^3$ respectively, given by the European Air Quality Directive 2008/50/EC [2, 3]. In addition to natural emissions, the large anthropogenic contributions of particles from local sources increase the level of PM₁₀ and micropollutants such as heavy metals. In this context, some metals are good tracers of local emissions [4]; therefore, the analysis of their presence in particulate matter at receptor sites may help in identifying point sources that affect the local air quality.

Three main groups of source apportionment techniques are usually reported in the literature [5]. The first group consists of source-receptor modelling by means of deterministic models. This approach is the most mathematically complex and requires high quality emission datasets from inventories or direct measurements of pollutants [6], to model the dispersion, transformation, transport and deposition of such contaminants [7]. The second group of models is based on the statistical evaluation of the pollutants measured at receptor sites. These methods have been widely applied in source apportionment studies of different environmental matrices such as rainwater [8], bulk deposition [9] and airborne particles [10]. Major components, trace metals and organic compounds are usually considered in this type of analysis where Chemical Mass Balance (CMB), Principal Component Analysis (PCA) and Positive Matrix Factorization (PMF) are the main techniques [5]. The third group consists of methods based on the evaluation of monitoring data, for example, the correlation of meteorological variables, such as wind direction, with the levels of air pollutants [11,

12]. Graphical methods based on the evaluation of trace metals and wind direction monitoring data may be used to identify their sources.

The relationship between the levels of single pollutants and the wind direction is usually reported by means of pollutant concentration roses, which are polar diagrams that show how air pollution depends on wind direction [13]. If an ambient air quality monitoring station is markedly influenced by a source of the pollutant measured, the pollutant concentration rose shows a peak towards the local source [13, 14]. Rose analysis is a commonly used tool in source apportionment on local scales [15, 16] and for identifying local point sources [11, 17, 18]. Pollutant concentration roses require highly time-resolved concentration data due to the variability of most meteorological parameters over a long sampling period. However, trace metal levels are usually determined in PM₁₀ samples that are collected in sampling periods of 24/48 hours. Different strategies have been used to solve this. Firstly, highly time-resolved particulate composition data can be obtained from direct measurement of the particles at the receptor sites by aerosol spectrometry (e.g., ATOFMS, Time-of-Flight Mass Spectrometer) and can be plotted against the average wind direction data [19]. A second option is to use low time-resolved metal concentration data (e.g., 24 hours) and highly time-resolved wind direction data (e.g., 1 hour). Cosemans et al. [20] used modified pollutant concentration roses to demonstrate that SO₂ reference roses calculated from hourly concentration and wind direction data are similar to those obtained from modified pollutant concentration roses computed by mathematical methods from 24 hours concentration data and 1 hour wind direction data. Gladtko et al. [21] used calculated PM₁₀ and metal concentration roses in an industrial area from 24 hours surplus concentration data and 0.5 hour wind direction data to allocate the individual shares of emitting facilities in an integrated steel plant; surplus concentration data were first obtained by subtracting the background levels of these pollutants measured in sites not directly affected by the point sources. A third approach is to use daily metal concentration data and hourly wind direction data for the calculation of the contribution of each wind sector to the measured concentrations of elements. Yatin et al. [22] calculated the fractional contribution of each wind sector to measured concentrations of the elements in an aerosol in Ankara (Turkey) to analyse possible source directions. In a later work, Qin and Oduyemi [23] identified the source direction that affects the PM₁₀ data in Dundee (UK) by comparing the average contributions of the wind sectors to the concentrations of the mass and chemical species with the average frequencies of wind direction.

In this paper, graphical methods based on the approach developed by Yatin et al. [22] and Qin and Oduyemi [23] were applied to the main urban sites in the Cantabria Region (Northern Spain), and then, the results were compared to those obtained from the radial diagrams created from computed pollutant concentration roses developed from 24 hours and 48 hours metal levels and hourly wind data. Santander Bay was selected as a case study to evaluate the influence of point sources on Mn levels at three receptor sites (Santander, Alto Maliaño and Guarnizo) by means of the methodology developed in this work.

2. Methodology

2.1. Study area

Cantabria is a small coastal region located in Northern Spain where the number of exceedances of daily PM₁₀ values in some urban areas was higher than the maximum number of times allowed in the 2008/50/EC Directive (35 per year).

The three studied urban areas are described below.

Santander Bay has an important industrial area that is primarily related to iron, steel and ferro-manganese alloys manufacturing. In this area, three monitoring sites were available. SANT (13°28'26''N, 3°47'47''W) is an urban background station located on the rooftop of the "E.T.S. de Ingenieros Industriales y de Telecomunicaciones" building near the Sardinero beaches zone in Santander, the most populated city of the region. GUAR (43°24'16''N, 3°50'31''W), located 7 km from Santander, is a point strongly influenced by a nearby ferro-manganese alloys production plant. Additionally, ALM (43°24'55''N, 3°50'5''W) data were obtained from CIMA [24], which is a temporary station located 1 km N of the same ferro-manganese alloys production plant between the SANT and GUAR sampling points.

The second urban area was Torrelavega, where the monitoring cabin, TORR (43°22'3''N, 4°2'34''W), was placed in Barreda town, an urban background site with traffic and industrial influences. The main industrial activities in this area include pulp and chemical plants with an intensive use of fossil fuels.

Finally, Castro Urdiales (CAST 43°22'56''N, 3°13'14''W) is a coastal town located 10 km NW of an important industrial site composed of a petrochemical plant, a fuel power station and some metallurgical plants.

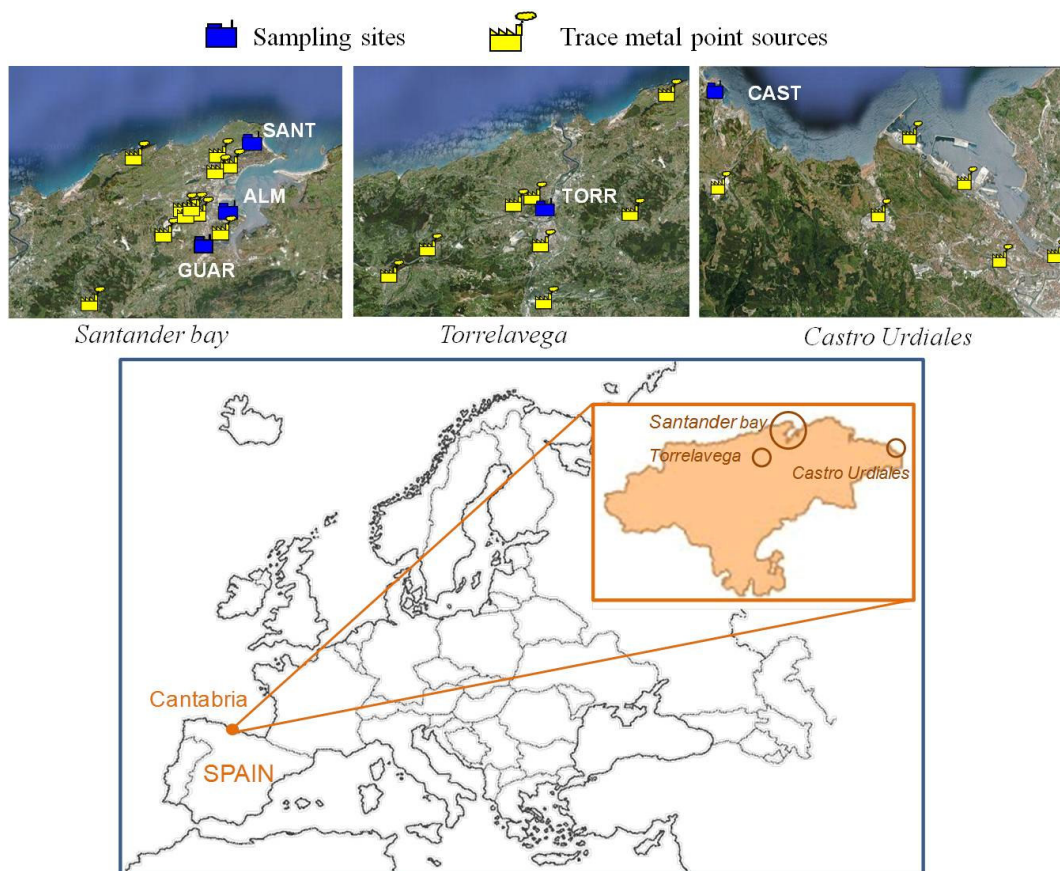


Figure 1. Location of the sampling sites and metals emitting point sources

Figure 1 shows the locations of the monitoring sites together with the main metals emitting sources situated nearby. The industrial sources of metals were obtained from the emission inventory provided by the European Pollutant Release and Transfer Register (e-PRTR).

2.2. Dataset

PM₁₀ sampling was carried out in 2008 and 2009 at the three urban areas to study the influence of industrial activity on the air quality of the region. PM₁₀ was collected for 24 hours in SANT on glass fiber filters (150 mm of diameter) by a high volume sampler (MCV, 30 m³/h). At the TORR, GUAR and CAST sites, 48 hours quartz micro-fiber filters (47 mm diameter, Sartorius) were collected by the Environmental Department of Cantabria Government using low volume samplers (2.3 m³/h). The analysis of the studied metals in the PM₁₀ samples was conducted by the UNE-EN 14902:2006 standard. Each filter was digested using a mix of HNO₃ and H₂O₂ in a microwave digestion system (ETHOS). Digested samples were analyzed by ICP-MS (Agilent 7500C). The blank contribution from the filters and reagents were evaluated and subtracted from the results. A minimum of 14% of the annual sampling period was selected for chemical analysis to fulfil the requirements of the air quality directive for indicative measurements (Directive 2004/107/EC). The datasets belonging to SANT, TORR and CAST in 2008 and to ALM in 2009 were published by Ruiz et al. [25] while the dataset related to GUAR during all the period and to SANT, TORR and CAST in 2009 are included for the first time in the present work.

Furthermore, the meteorological parameters, including wind direction and wind speed, from ALM, GUAR, TORR and CAST were supplied by the Air Quality Monitoring Network of the Regional Environmental Ministry of the Cantabrian Government, while the values corresponding to SANT were provided by the Meteorological State Agency (AEMET) and were taken from a monitoring station 2 km away.

2.3. Procedure for the evaluation of trace metal levels and wind data

The contribution of each wind sector to the measured concentrations of trace elements may show the possible source direction. Yatin et al. [22] calculated the fractional contribution of each wind sector to the measured concentrations of PM-bound elements in Ankara, Turkey, to analyse the possible source direction. Additionally, Qin and Oduyemi [23] roughly identified the possible source direction that affects PM10 data in Dundee, UK, by comparing the average contributions of the wind sectors to the concentrations of the mass and chemical species with the average frequencies of the wind direction. The average contributions of the wind sectors to the concentrations can be calculated by using:

$$E_{jk} = \sum_{i=1}^N C_{ik} \cdot P_{ij} / \sum_{i=1}^N C_{ik} \quad (1)$$

where

E_{jk} : the average contribution of wind direction j to chemical species k (%)

C_{ik} : the concentration of chemical species k in sample i

P_{ij} : the frequency of wind direction j during the period of sample i (%)

N : the number of samples.

The average contribution of the wind sector to a chemical species (E_{jk}) could be higher than the average wind direction frequency (AWF), which means the contribution of the source from this direction to this species is higher than the average level and the source will strongly contribute to this species in this direction. Conversely, when the average contribution of the wind sector to a chemical species (E_{jk}) is lower than the wind direction frequency, the contribution of the source from this direction to this species will be lower than the average level, and the source contribution to this species will be weak in this direction [23]. In this work, the average distributions of wind direction frequency (AWF) and the average contributions of wind sector to each trace element (E_{jk}) are represented by polar diagrams to improve the discussion of the contribution of the sources in the studied area.

There are other graphical methods that could be used to evaluate trace metal levels and wind data. In the present work, computed pollutant concentration roses based on the methodology developed by Cosemans and Kretzschmar [26] were chosen. When the pollutant data are averaged over 24 hours, as is the case of heavy metals, the construction of a pollutant concentration rose requires a mathematical methodology to obtain high quality plots as shown in equation (2). The computed pollutant concentration rose is a vector with a dimension equal to the number of sectors used, in this case 36.

$$c_i = \sum_{j=1,n} p_j \cdot f_{i,j} \cdot \alpha_j / \sum_{j=1,n} f_{i,j} \cdot \alpha_j$$

(2)

Where:

j : day index for the period under investigation.

n : the number of days in the period for which the rose is constructed.

i : the wind sector index for the rose. (1-36 for sectors of 10°).

c_i : the resulting average concentration for wind sector i in the studied period.

p_j : the measured concentration on day j .

$f_{i,j}$: the number of hours that the wind came from sector i on day j .

α_j : some weight function based on the persistency of the wind vector during day j .

In this case, α_j is set to the inverse of the number of wind direction bins on day j with non-zero frequency, n_j .

$$\alpha_j = 1/n_j \quad (3)$$

This means that if the wind pattern of a given day is well distributed, n_j will be high (the maximum value would be 24), and α_j will be small. Therefore, the wind dispersion of this day will lead to a small weight of the pollutant concentration. On the other hand, when wind blows only from one or two sectors on a given day, α_j will be higher, so the weight of the pollutant concentration will be higher. A similar procedure was followed for the samples that were collected for 48 hours.

3. Results and discussion

3.1. Trace metal concentrations

In a previous study the following elements were highlighted as marker species for the different emissions sources identified in each studied area: Mn in Santander Bay, Cu and Cr in Torrelavega and Ni and V in Castro Urdiales [25]. The mean, standard deviation, and maximum and minimum concentrations of these trace metals in the PM10 at the SANT, ALM, GUAR, TORR and CAST sites are shown in Table 1.

Table 1. Mean (M), standard deviation (S.D.), and minimum (Min) and maximum (Max) levels of the studied tracers (ng/m^3). N is the number of samples.

Site	Tracer	Year	M	S.D.	Max	Min	N
SANT*	Mn	2008	49.1	60.8	242.0	<1.8	50
		2009	31.5	43.5	201.7	<1.8	45
ALM*(1)	Mn	2009	1,071.7	1,436.5	8,859.9	<0.9	108
GUAR**	Mn	2008	160.4	158.8	514.9	6.5	28
		2009	118.0	169.4	587.2	2.0	28
TORR**	Cu	2008	18.9	10.5	44.9	<1.1	29
		2009	18.8	11.4	56.9	3.0	26
	Cr	2008	25.8	58.8	285.6	<2.3	29
		2009	3.4	3.1	13.8	<3.3	26
CAST**	Ni	2008	3.0	2.7	12.8	1.0	28
		2009	3.4	2.8	11.7	0.7	26
	V	2008	3.1	3.7	19.1	0.1	28
		2009	4.4	4.0	13.3	0.4	26

* These statistical values are calculated from concentrations of 24 hours samples

** These statistical values are calculated from concentrations of 48 hours samples

(1) The ALM data are from samples collected in 2009 [24]

Mn is the main industrial tracer identified in Santander Bay. A decreasing trend in the Mn level can be observed in Table 1, and is attributed to the impact of the economic crisis on the Cantabria metallurgical industry in 2009, as reported by Arruti et al. [27]. Two tracers were used at the TORR site, Cu and Cr. Cu, which is linked to traffic emissions, presents unchanged levels during all of the studied period, while Cr, a typical combustion tracer, experienced a reduction in 2009. Ni and V are typical tracers of the petrochemical industry [28], so these metals were selected as markers at the CAST site because a petrochemical plant is located near this town. A high correlation ($r=0.87$, $p<0.01$) between the levels of these metals has been obtained, which supports the idea that this plant is their major source. Moreover, CO_2 emissions from the petrochemical plant in 2008 and 2009, as published by e-PRTR, indicate that its production was maintained throughout the period, which could explain why the levels of both tracers did not decrease in 2009.

As expected, Mn concentrations measured in ALM and GUAR are higher than the levels found in other Spanish areas affected by steel manufacturing [29], which could be explained by the influence of the nearby ferro-manganese and silico-manganese factory [25, 30, 31]. The rest of the selected metals are in the range of other Spanish urban sites [29]. Finally, among the studied tracers, Ni is the only trace metal with an annual target value in the EU Air Quality Directives ($20 \text{ ng}/\text{m}^3$) and this value was not exceeded in any of the samples.

3.2. Graphical procedures for identifying the contribution of sources

The average contributions of wind directions to Ni and V concentrations in CAST and to Cu and Cr concentrations in TORR as calculated according to equation (1) are plotted

in polar diagrams together with AWF (Figure 2a). Figure 2b represents the ratio between the average contribution of each wind direction to the respective trace metal, $E_{j,k}$ ($E_{j,Ni}$ and $E_{j,V}$ for CAST and $E_{j,Cu}$ and $E_{j,Cr}$ for TORR), and AWF. Next, Figure 2c shows the roses of the trace metals selected for each site, which were computed from the methodology developed by Cosemans and Kretzschmar [26], according to equation (2).

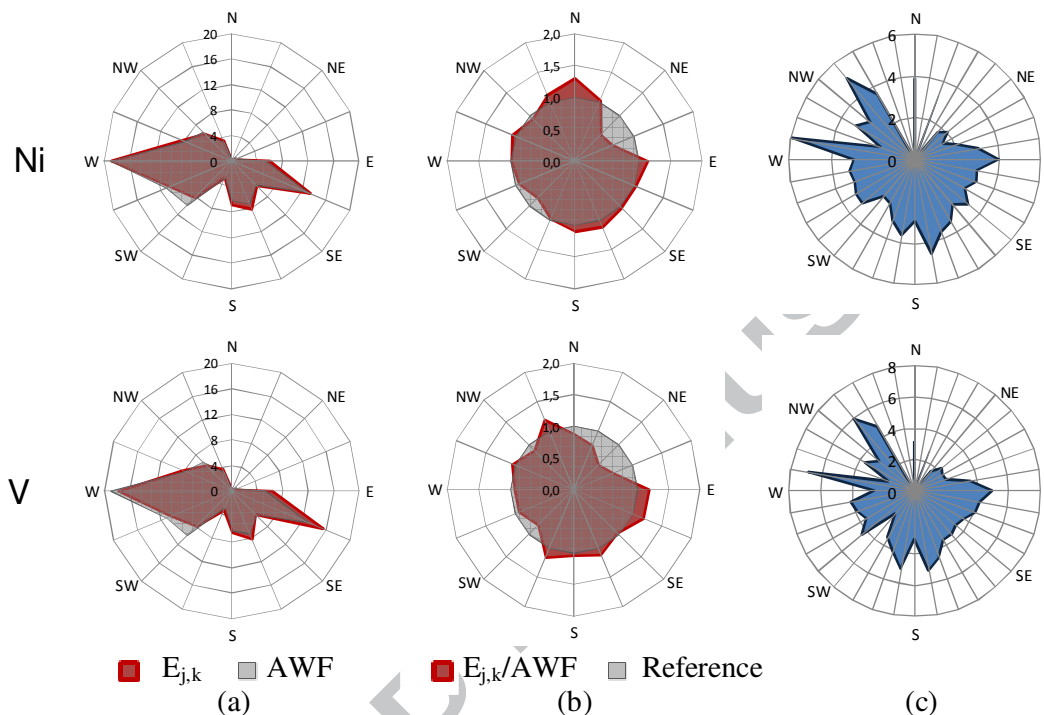


Figure 2. Graphical procedures based on the evaluation of Ni and V levels and wind direction data at CAST for 2008-2009: a) $E_{j,k}$ (%) and AWF (%); b) $E_{j,k}/AWF$ ratio; c) computed roses (ng/m^3) from Cosemans and Kretzschmar [26].

The two ways to represent the average contributions of wind directions to metal concentrations in polar diagrams offer a discussion about the profiles obtained that when the wind contribution plays an important role. When $E_{j,k}$ and AWF are plotted together and practically overlap (see Ni and V in Figure 2a and Cu in figure 3a), a plot of the $E_{j,k}/AWF$ ratio simplifies the interpretation of the results (see Ni and V in Figure 2b and Cu in figure 3b). In the case of Cr, similar conclusions can be obtained from both polar diagrams because $E_{j,Cr}$ is clearly higher than AWF in the SW-W sector, as shown in Figures 3a and 3b.

When these polar diagrams are compared to the pollutant concentration roses computed from the procedure developed by Cosemans and Kretzschmar [26], similar conclusions were obtained for V and Ni from the CAST site and for Cu from the TORR site, with some exceptions. In figure 2c, some peaks for V and Ni are pointing in the W and NW directions, which have been identified as a ‘false’ peak due to the absence of pollutant sources in this direction. The predominance of this wind direction can be observed in figure 2a, while these peaks are not presented in figure 2b where the influence of wind frequency was attenuated. However, the Cr rose (Figure 3c) leads to a different interpretation when it is compared to the other polar diagrams (Figure 3a and b). Figure 3b is the plot that best represents the influence of the main sources (the industrial

combustion facilities located 1 km W of the sampling site), while Figure 3c does not show clear conclusions owing to its uniform profile. Furthermore, a ‘false’ N-NE peak appears where no Cr sources are located.

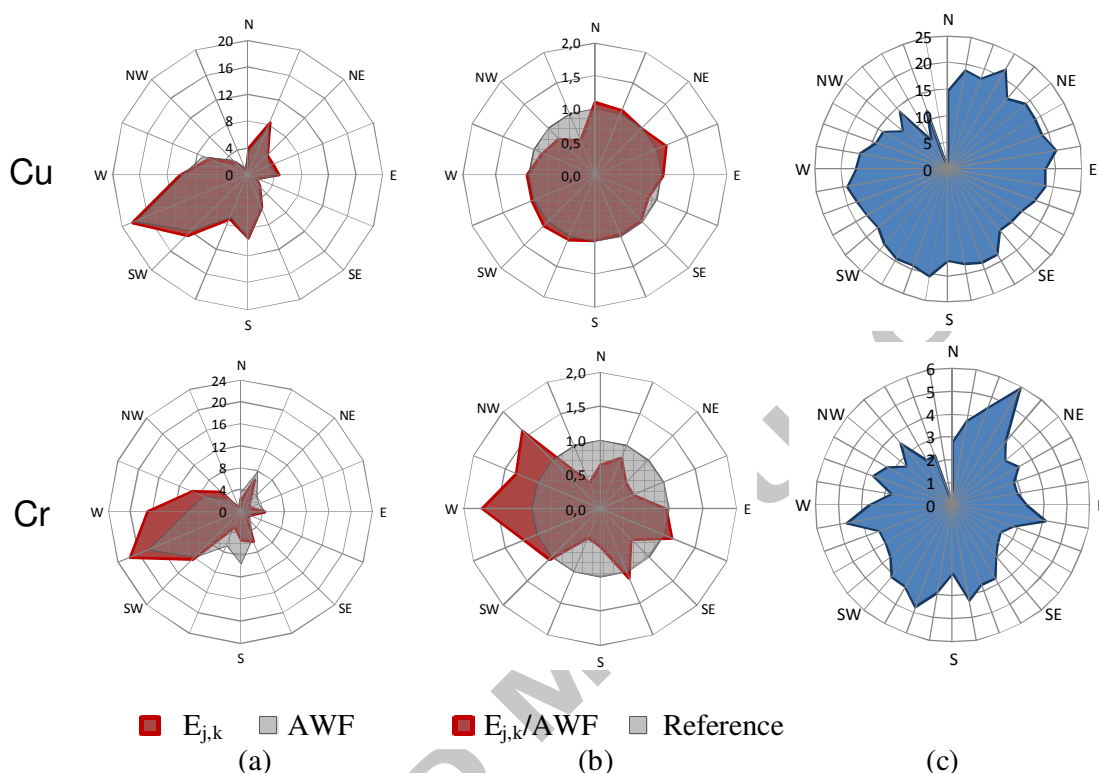


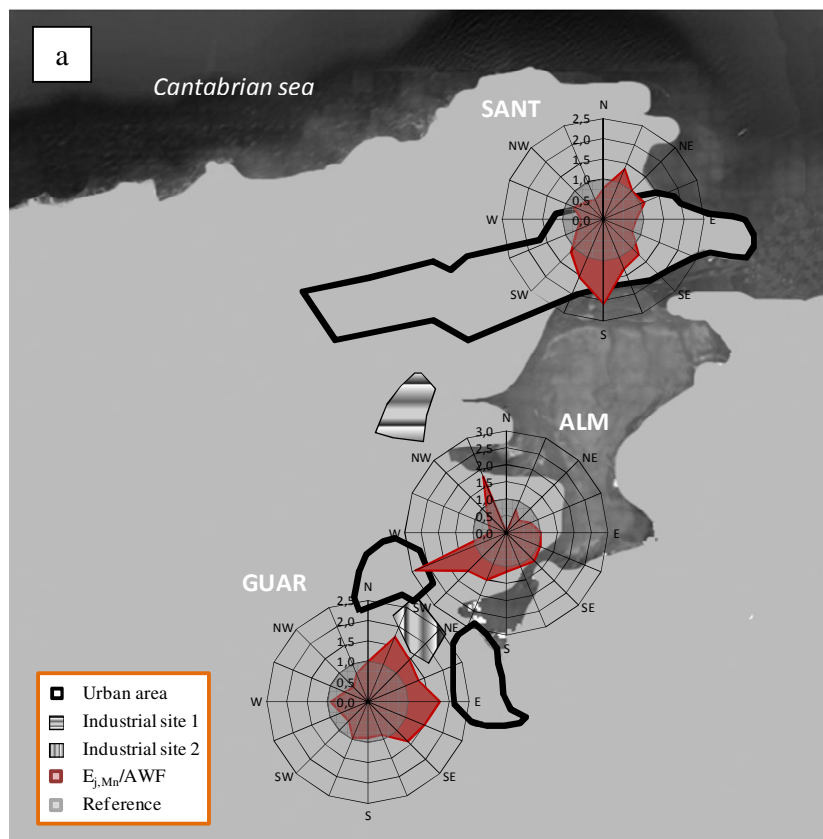
Figure 3. Graphical procedures based on the evaluation of Cu and Cr levels and wind direction data at TORR for 2008-2009: a) $E_{j,k}$ (%) and AWF (%); b) $E_{j,k}/AWF$ ratio; c) computed roses (ng/m^3) from Cosemans and Kretzschmar [26].

With respect to the influence of the point sources on the levels of the other studied metals, Figure 2 shows similar behaviour of Ni and V at the CAST site. The higher contributions of Ni and V are associated with sectors from the east to the south (see Figure 2b), where the petrochemical plant is located. On the other hand, the uniformity of the Cu polar diagrams from the TORR site (figures 3b and c) may be explained by the traffic contribution from all sectors around the sampling site.

3.3. Application of pollutant polar diagrams to a case study: Santander Bay

The proposed methods show some limitations when different sources with relatively low intensity are located in the study area. Therefore, this procedure is applied to the case of Mn in Santander Bay, where large Mn point sources are located within a relatively short distance. $E_{j,k}/AWF$ diagrams have been chosen to plot the Mn levels in Santander Bay because they provide the easiest way to interpret the influence of point sources on the levels of pollutants at a given receptor site (figure 4a). Santander Bay was chosen as a case study because three sampling sites, located at different distances from the two main Mn point sources, were available: SANT, ALM and GUAR. Figure 4 shows the locations of the most important Mn point sources: industrial site 1, where a

non-integrated steel plant and an iron foundry are found; and industrial site 2, where a ferro-manganese and silico-manganese plant is located. Computed roses from the procedure developed by Cosemans and Kretzschmar [26] were also plotted in the same area (figure 4b).



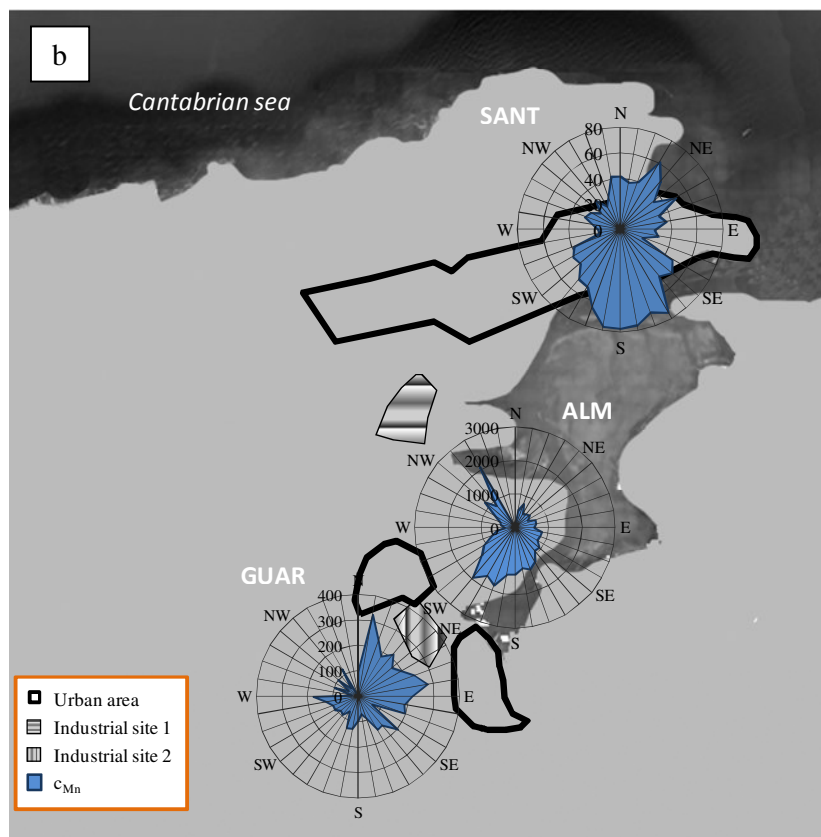


Figure 4. Polar diagrams of Mn in Santander Bay a) $E_{j,Mn}/AWF$ ratio; b) computed roses (ng/m^3) from Cosemans and Kretzschmar [26].

The comparison of radial diagrams of $E_{j,Mn}/AWF$ ratios and the computed Mn roses based on the procedure developed by Cosemans and Kretzschmar [26] leads to similar results, with both figures indicating that the main contribution to the Mn levels comes from the S-SW in SANT, from the SW in ALM and from the N-NE in GUAR, where ferro-manganese and silico-manganese alloys are produced. However, these computed roses take into account the intensity of the sources, because the concentration of Mn in each sector is represented in the polar diagrams; thus, a maximum peak of $2000 \text{ ng}/\text{m}^3$ is observed in ALM, which is only 500 m away from two of the ferroalloys furnaces; in GUAR and SANT, the maximum Mn peaks were approximately 300 and $80 \text{ ng}/\text{m}^3$ respectively. These sites are 1 and 7.5 km away from the ferroalloy plant, respectively. A peak pointing to the NW was also found at the ALM site, where industrial site 1 is located; the steel production by electric arc furnaces (EAF) and the iron foundry are possible sources of the Mn, although the concentration of Mn in EAF and foundry dust is usually low, between 1.5 and 3.5 wt % [32]. In addition, both diagrams present a peak in the NE sector of SANT, most likely owing to the characteristic NE sea breeze that appears in the afternoon. This characteristic wind pattern is shown in Figure 5, where the morning and afternoon wind roses recorded in Santander Bay are plotted. Thus, light winds blow predominantly from the SW in the morning (see Figure 5a), but in the afternoon, they reverse direction to become moderate NE onshore breezes (see Figure 5b), which return the industrial pollution plume inland [30], thus raising the Mn concentration in NE sector, primarily at the SANT sampling site. Therefore, it is important to have "a priori" information about the sources to correctly interpret the

peaks shown in these polar diagrams, particularly when the influence of local wind patterns, such as sea breezes, may produce unexpected peaks.

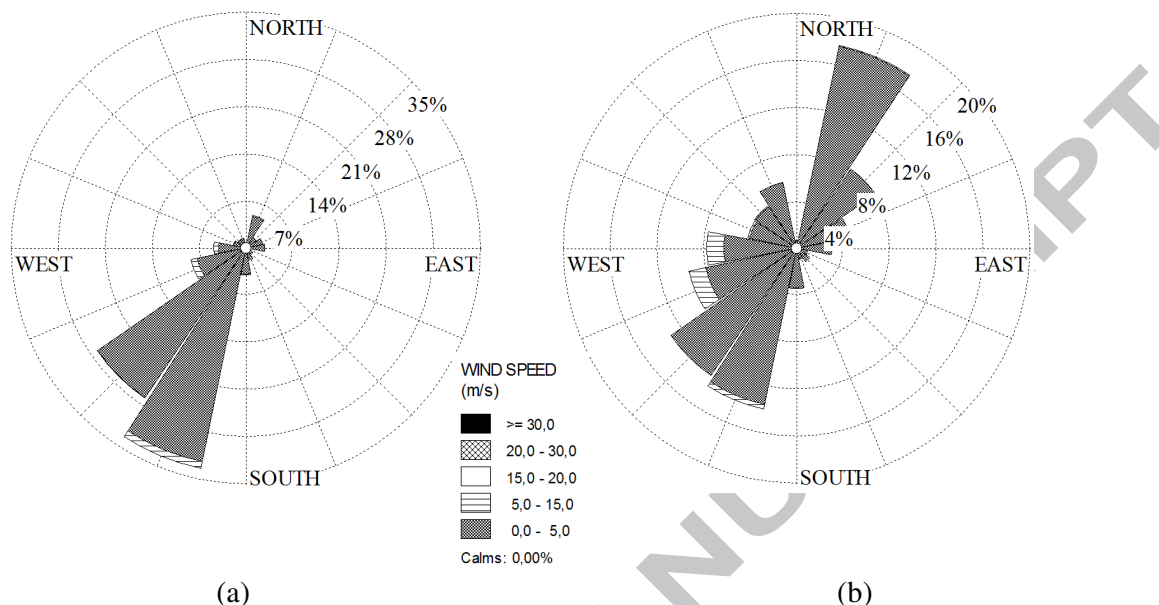


Figure 5. Wind roses in GUAR for 2008-2009: a) in the morning and b) in the afternoon.

4. Conclusions

Different trace metals were identified as tracers of nearby industrial activities at three mixed urban/industrial sites in the Cantabria Region: Mn in Santander Bay, V and Ni in Castro Urdiales and Cu and Cr in Torrelavega. Graphical methods using wind direction data and metal levels based on the approach developed by Qin and Oduyemi [23] were compared to those obtained from the computed pollutant concentration roses developed by a methodology proposed by Cosemans and Kretzschmar [26] to identify local sources of these tracers. The simultaneous plotting of the average contributions of wind directions to metal concentration ($E_{j, \text{tracer}}$) with the average wind frequency (AWF) can be considered a valid procedure except when both plots practically overlap; in these cases, the polar diagrams may be improved when the $E_{j, \text{tracer}}/\text{AWF}$ ratios are applied. This procedure based on polar diagrams of $E_{j, \text{tracer}}/\text{AWF}$ ratios, may result in an easier interpretation of the data. Moreover, some 'false' peaks appear in the sectors with very low wind frequencies when computed roses were used. Finally, Santander Bay was chosen as a case study to discuss the ability of the $E_{j, \text{tracer}}/\text{AWF}$ plots and the pollution roses to recognise point sources affecting the levels of some metals (e.g., Mn) at different receptor sites. The analysis of the results shows that similar conclusions were obtained from both methods in the studied area: the strong influence of the manganese alloys production plant, the lower impact of other Mn emitting sources such as steel manufacturing and iron foundries, and the important influence of the NE afternoon sea breeze at the coastal site, which returns the Mn pollution plume inland. The proposed method is recommended when large emissions are produced by local point sources. When diffuse or fugitive sources such as small industrial complexes, vehicular or residential sources are characteristic in the study area, the proposed graphical methods should be used with caution.

References

- [1] C.A. Pope III and D.W. Dockery, Health effects of fine particulate air pollution: lies that connect, *J. Air Waste Manag. Assoc.* 56 (2006) 709-742.
- [2] X. Querol, A. Alastuey, T. Moreno, M.M. Viana, S. Castillo, J. Pey, S. Rodríguez, B. Artiñano, P. Salvador, M. Sánchez, S. García Dos Santos, M.D. Herce Garraleta, R. Fernández-Patier, S. Moreno-Grau, L. Negral, M.C. Minguillón, E. Monfort, M.J. Sanz, R. Palomo-Marín, E. Pinilla-Gil, E. Cuevas, J. de la Rosa, A. Sánchez de la Campa, Spatial temporal variations in airborne particulate matter PM10 and PM2.5 across Spain 1999-2005, *Atmos. Environ.* 42 (2008) 3964-79.
- [3] J.P. Putaud, R. Van Dingenen, A. Alastuey, H. Bauer, W. Birmili, J. Cyrys, H. Flentje, S. Fuzzi, R. Gehrig, H.C. Hansson, R.M. Harrison, H. Herrmann, R. Hitzenberger, C. Hüglin, A.M. Jones, A. Kasper-Giebl, G. Kiss, A. Koussa, T.A.J. Kuhlbusch, G. Löschau, W. Maenhaut, A. Molnar, T. Moreno, J. Pekkanen, C. Perrino, M. Pitz, H. Puxbaum, X. Querol, S. Rodriguez, I. Salma, J. Schwarz, J. Smolik, J. Schneider, G. Spindler, H. ten Brink, J. Tursic, M. Viana, A. Wiedensohler, F. Raes, A European aerosol phenomenology – 3: Physical and chemical characteristics of particulate matter from 60 rural, urban, and kerbside sites across Europe, *Atmos. Res.* 44 (2010) 1308-1320.
- [4] T. Moreno, X. Querol, A. Alastuey, M. Viana, P. Salvador, A. Sánchez de la Campa, B. Artiñano, J. de la Rosa, W. Gibbons, Variations in atmospheric PM trace metal content in Spanish towns: Illustrating the chemical complexity of the inorganic urban aerosol cocktail, *Atmos. Environ.* 40 (2006) 6791-6803.
- [5] M. Viana, T.A.J. Kuhlbusch, X. Querol, A. Alastuey, R.M. Harrison, P.K. Hopke, W. Winiwarter, M. Vallius, S. Szidat, A.S.H. Prévôt, C. Hueglin, H. Bloemen, P. Wahlin, R. Vecchi, A.I. Miranda, A. Kasper-Giebl, W. Maenhaut, R. Hitzenberger, Source apportionment of particulate matter in Europe: a review of methods and results, *Aerosol Sci. Technol.* 39 (2008) 827-849.
- [6] J. Maes, J. Vliegen, K. Van de Vel, S. Janssen, F. Deutsch, K. de Redder, C. Mensink, Spatial surrogates for the disaggregation of CORINAIR emission inventories, *Atmos. Environ.* 43 (2009) 1246-1254.
- [7] B. Bessagnet, A. Hodzic, R. Vautard, M. Beekmann, S. Cheinet, C. Honoré, C. Liousse, L. Rouil, Aerosol modeling with CHIMERE - Preliminary evaluation at the continental scale, *Atmos. Environ.* 38 (2004) 2803-2817.
- [8] S. Juntto and P. Paatero, Analysis of daily precipitation by positive matrix factorization, *Environmetrics* 5 (1994) 127-144.
- [9] Z. Mijic, A. Stojic, M. Perisic, S. Rajsic, M. Tasic, M. Radenkovic, J. Joksic, Seasonal variability and source apportionment of metals in the atmospheric deposition in Belgrade, *Atmos. Environ.* 44 (2010) 3630-3637.
- [10] M. Pandolfi, M.Viana, M.C. Minguillón, X. Querol, A. Alastuey, F. Amato, I. Celades, A. Escrig, E. Monfort, Receptor models application to multiyear ambient

- PM10 measurement in an industrialized area: comparison of source apportionment results, *Atmos. Environ.* 42 (2008) 9007-9017.
- [11] R.C. Henry, Y.-S. Chang, C.H. Spielgelman, Locating nearby sources of air pollution by nonparametric regression of atmospheric concentrations on wind direction, *Atmos. Environ.* 36 (2002) 2237-2244.
- [12] M.C. Somerville, S. Mukerjee, D.L. Fox, Estimating the wind directions of maximum air pollutant concentration, *Environmetrics* 7 (1996) 231-243.
- [13] P.H.C. Eilers, Penalized regression in action: estimating pollution roses from daily averages, *Environmetrics* 2 (1991) 25-47.
- [14] G. Cosemans, J. Kretzschmar, Pollutant roses for 24h averaged pollutant concentrations by respectively least squares regression and weighted, 9th Conf. On Harmonisation within Atmospheric Dispersion Modelling for Regulatory Purposes, 2004.
- [15] P. Lenschow, H.-J. Abraham, K. Kutzner, M. Lutz, J.-D. Preuß, W. Reichenbacher, Some ideas about the sources of PM10, *Atmos. Environ.* 35 (2001) Supplement No. 1, S23-S33.
- [16] M. Rigby, R. Timmis, R. Toumi, Similarities of boundary layer ventilation and particulate matter roses, *Atmos. Environ.* 40 (2006) 5112-5124.
- [17] R. Fernández-Camacho, J. de la Rosa, A.M. Sánchez de la Campa, Y. González-Castanedo, A. Alastuey, X. Querol, S. Rodríguez, Geochemical characterization of Cu-smelter emission plumes with impact in an urban area of SW Spain, *Atmos. Res.* 96 (2010) 590-601.
- [18] M.C. Somerville, S. Mukerjee, D.L. Fox, R.K. Stevens, Statistical approaches in wind sector analyses for assessing local source impacts, *Atmos. Environ.* 28 (1994) 3483-3493.
- [19] D.C. Snyder, J.J. Schauer, D.S. Gross, J.R. Turner, Estimating the contribution of point sources to atmospheric metals using single-particle mass spectrometry, *Atmos. Environ.* 43 (2009) 4033-4042.
- [20] G. Cosemans, J. Kretzschmar, C. Mensink, Pollutant roses for daily averaged ambient air pollutant concentrations, *Atmos. Environ.* 42 (2008) 6982-6991.
- [21] D. Gladtko, W. Volkhausen, B. Bach, Estimating the contribution of industrial facilities to annual PM10 concentrations at industrially influenced sites, *Atmos. Environ.* 43 (2009) 4655-4665.
- [22] M. Yatin, S. Tuncel, N.K. Aras, I. Olmez, S. Aygun, G. Tuncel, Atmospheric trace elements in Ankara, Turkey: 1. Factors affecting chemical composition of fine particles, *Atmos. Environ.* 34 (2000) 1305-1318.

- [23] Y. Qin, K. Oduyemi, Chemical composition of atmospheric aerosol in Dundee, UK, *Atmos. Environ.* 37 (2003) 93-104.
- [24] CIMA (Government of Cantabria), Evaluación de la calidad del aire y analítica de metales en la fracción PM10 en el Alto Maliaño, Internal report C-077/2008 (2010).
- [25] S. Ruiz, A. Arruti, I. Fernández-Olmo, J.A. Irabien, Contribution of point sources to trace metal levels in urban areas surrounded by industrial activities in the Cantabria Region (Northern Spain), *Procedia Environ. Sci.* 4 (2011) 76-86.
- [26] G. Cosemans, J. Kretzschmar, Pollution roses for 24h averaged pollutant concentrations by regression, 8th Conf. on Harmonisation within Atmospheric Dispersion Modelling for Regulatory Purposes, Sofia, Bulgaria, 14-17 Oct. 2002, E. Batchvarova and D. Syrakov (Eds.), ISBN 954-9526-12-7, pp. 414 - 418.
- [27] A. Arruti, I. Fernández-Olmo, A. Irabien, Impact of the global economic crisis on metal levels in particulate matter (PM) at an urban area in the Cantabria Region (Northern Spain), *Environ. Pollut.* 159 (2011) 1129-1135.
- [28] M.L. Bosco, D. Varriaca, G. Dongarrà, Case study: Inorganic pollutants associated with particulate matter from an area near a petrochemical plant, *Environ. Res.* 99 (2005) 18-30.
- [29] X. Querol, M. Viana, A. Alastuey, F. Amato, T. Moreno, S. Castillo, J. Pey, J. de la Rosa, A. Sánchez de la Campa, B. Artíñano, P. Salvador, S. García Dos Santos, R. Fernández-Patier, S. Moreno-Grau, L. Negral, M.C. Minguillón, E. Monfort, J.I. Gil, L.A. Ortega, J.M. Santamaría, J. Zabalza, Source origin of trace elements in PM from regional background, urban and industrial sites in Spain, *Atmos. Environ.* 41 (2007) 7219-7231.
- [30] T. Moreno, M. Pandolfi, X. Querol, J. Lavín, A. Alastuey, M. Viana, W. Gibbons, Manganese in the urban atmosphere: identifying anomalous concentrations and sources, *Environ. Sci. Pollut. Res.* 18 (2011) 173-183.
- [31] A. Arruti, I. Fernández-Olmo, A. Irabien, Regional evaluation of particulate matter composition in an Atlantic coastal area (Cantabria region, northern Spain): Spatial variations in different urban and rural environments, *Atmos. Res.* 101 (2011) 280-293.
- [32] EPA (U.S. Environmental Protection Agency), Locating and estimating air emissions from sources of manganese, EPA-450/4-84-007h. September, 1985.

Acknowledgments

The authors are thankful for the financial support from the CTM 2010-16068 project (Spanish Ministry of Science and Innovation). The authors would also like to thank the Regional Environment Ministry of the Cantabria Government for providing the PM10 samples at the GUAR, CAST and TORR sites, and the Meteorological State Agency (AEMET) for supplying the wind information at SANT.

ACCEPTED MANUSCRIPT

Highlights

Trace metals in particulate matter as markers of industrial point sources

Graphical methods based on metal levels and wind data to identify point sources

Average contributions of the wind sectors to tracer levels plotted in polar diagrams

Computed metal roses for 24/48 h samples also provide high quality plots of tracers

ACCEPTED MANUSCRIPT